Methods to Determine Solubility Parameters of Polymers at High Temperature Using Inverse Gas Chromatography

Jan-Chan Huang

Plastics Engineering Department, University of Massachusetts Lowell, Lowell, Massachusetts 01854, USA

ABSTRACT: Experimental values of Flory–Huggins parameters, χ, between polymers and probes, are frequently used to determine the solubility parameters of the polymers by the method of DiPaola–Baranyi and Guillet. The solubility parameters of probes were usually estimated by using heat of vaporization. When χ is measured at a temperature near the critical temperature of the probes and used to determine the solubility parameter of polymers, the departure of enthalpy of the probe vapor from the ideal gas state should be considered. This study discussed the method to make the correction and its effect on the determination solubility parameter of polymers. Without correction in the vapor phase enthalpy, the solubility parameters of the probes and polymer tend to be underestimated and the error increases when the critical temperature is approaching. Analytical expressions for the effect of correction on the solubility parameter of probes and parameters of polymers were derived. By use of probes with a range of solubility parameters on both sides of the solubility parameter of polymers, the correlation between parameters of polymers was shown to be reduced. © 2004 Wiley Periodicals, Inc. J Appl Polym Sci 94: 1547–1555, 2004

Key words: chromatography; thermodynamics solution properties; solubility parameter; enthalpy

INTRODUCTION

The knowledge of the interaction parameters between polymers and solvents is very important in the study of their miscibility and thermodynamic properties of solutions. Inverse gas chromatography (IGC) was demonstrated to be an effective tool for measuring the thermodynamic properties of solute (probe) vapors in polymers.[1–4] The name IGC was used because the subject of the study is the stationary phase rather than the probes. In IGC measurement, a known amount of nonvolatile stationary phase is dissolved in a solvent and coated on a porous inert support. When a liquid probe is injected into the column, the probe vaporizes and flows with the carrier gas, and a characteristic specific retention volume can be measured. If the molecular weight of the stationary phase is known, the specific retention volume can be related to the activity coefficient of the probe in the stationary phase.[1–7] By using Flory–Huggins theory,[8] the Flory–Huggins interaction parameter between a polymer and probe, χ, can be related to the specific retention volume of probes, V_g^0, by[1–5]

$$\chi = \ln\left(\frac{273.16Rv_2}{V_g^0 P_1^0 V_1}\right) - 1 + \frac{V_1}{M_2 v_2} - \frac{P_1^0}{RT}(B_{11} - V_1) \quad (1)$$

Correspondence to: Jan_Huang@uml.edu.

where R is the gas constant, T is the column temperature, v_2 is the specific volume, M_2 is the molecular weight of the stationary phase, and P_1^0, V_1, and B_{11} are the vapor pressure, liquid molar volume, and the second viral coefficient of the probe, respectively. In the IGC study of polymers, the molecular weight M_2 is large; the $V_1/M_2 v_2$ term is usually small and can be neglected. When $\chi < 0.5$, the probe liquid is generally characterized as a good solvent for the polymer, whereas a value > 0.5 is a poor solvent and may lead to phase separation.[8] IGC was first applied by Guillet and coworkers[9,10] to study the thermodynamics of probe–polymer interactions by using a polymer as the stationary phase. The interaction between probes and a polymer is usually represented by the Flory–Huggins interaction parameters, χ, and analyzed through the solubility parameters of the polymer and probes.

METHOD TO DETERMINE THE SOLUBILITY PARAMETER

In 1916, Hildebrand[11] pointed out that the relative solubility of a given solute in a series of solvents is determined by the internal pressures of the solvents. Later, Scatchard[12] introduced the concept of cohesive energy density into Hildebrand's theory, identifying this quantity to be the internal pressure. In 1949, Hildebrand proposed the term solubility parameter and the symbol δ, which is defined as the square root of the cohesive energy density[13]

$$\delta = \left(\frac{\Delta E_{\mathrm{vap}}}{V}\right)^{1/2} = \left(\frac{\Delta H_{\mathrm{vap}} - RT}{V}\right)^{1/2} \quad (2)$$

where ΔE_{vap} and ΔH_{vap} are the energy and enthalpy of vaporization, respectively, and V is the molar volume of the liquid. The cohesive energy density represents the energy required to separate the liquid molecules into the ideal gas state. In the above equation, it was assumed that the vapor phase is an ideal gas; therefore, $\Delta E = \Delta H - PV = \Delta H - RT$. An unambiguous value of solubility parameter can be determined if the material can be vaporized. The heat of vaporization is frequently calculated from the vapor pressure of the saturated liquid by the Clausius–Clapeyron equation:

$$\frac{d \ln P}{d(1/T)} = -\frac{\Delta H_{\mathrm{vap}}}{R\Delta Z} \quad (3)$$

where ΔZ is the difference in the compressibility factor between the saturated vapor and saturated liquid. It is unity when the gas phase is in an ideal gas state and the compressibility factor of the probe liquid is small, but will be less than unity when temperature approaches the critical temperature.

The solubility parameter model was successful in describing thermodynamic properties of solutions. It was shown that the Flory–Huggins interaction parameter can be related to the solubility parameters of the two components by the relation[13]

$$\chi = (V_1/RT)(\delta_1 - \delta_2)^2 \quad (4)$$

where δ_1 and δ_2 are the solubility parameters of the probe and the polymer, respectively, and V_1 is the volume of the probe. The above equation implies that χ is always positive. A negative experimental value of χ can occur in systems with a specific interaction. One way to overcome this problem is to add an entropy term into the Flory–Huggins interaction parameter so that $\chi = \chi_H + \chi_S$,[14–18] where the dimensionless χ_S is an entropy term which can be used to accommodate deviation from the original solubility parameter model in eq. (4). When χ_S is added, the following modified form of the solubility parameter model is obtained

$$\chi = (V_1/RT)(\delta_1 - \delta_2)^2 + \chi_S \quad (5)$$

Because polymers have no appreciable vapor pressure and their molar volumes are not accurately known, the definition in eqs. (2) and (3) cannot be used for polymers. Experimental values of χ were used in the determination of the solubility parameters of polymers. Guillet et al.[14,15] demonstrated the use of IGC in the determination of χ and the solubility parameters of polymers. In their studies,[14,15] eq. (5) was modified as

$$\left(\frac{\delta_1^2}{RT} - \frac{\chi}{V_1}\right) = \left(\frac{2\delta_2}{RT}\right)\delta_1 - \left(\frac{\delta_2^2}{RT} + \eta\right) \quad (6)$$

where $\eta = \chi_S/V_1$. In the application of eq. (6) to IGC data, it is assumed that the η term depends on the polymer and remains constant for a series of probes. The expression then has a form similar to a linear equation with the slope. From the standard formula of the linear least-squares method, the expression of δ_2 was derived in a previous study to be[19]

$$\delta_2 = [\Sigma(\delta_i - \bar{\delta})(\delta_i^2 - RT\chi_i/V_i)]/2[\Sigma(\delta_i - \bar{\delta})^2] \quad (7)$$

After δ_2 is determined from the slope term, the intercept is used to calculate η. From χ, δ_i, and δ_2, the values of χ_S for each probe are determined by using eq. (5).[14,15,20,21] Guillet et al.[14] determined χ_S by using the above approach for hydrocarbon probes in ethylene–propylene rubber, cis-polyisoprene, and amorphous polypropylene. The values were ~ 0.3 and showed a small probe dependence; they were higher for linear alkanes and smaller for aromatic probes. Since then many studies[20–26] were made to determine the solubility parameters of polymers, a collection of studies of the Flory–Huggins interaction parameters and solubility parameters of polymers was published by Barton.[27]

IGC was used for high temperature starting from the early study of DiPaola-Baranyi and Guillet.[14] In that study, temperatures up to 203°C were used to measure χ in polystyrene. In the case of polymers with a high glass transition temperature such as poly(2,6-dimethyl-1,4-phenylene oxide), temperatures as high as 280°C were used.[28] It is a recent trend that IGC is used to measure the solubility parameters of polymers at high temperatures.[29–33] Some common probes such as hexane, benzene, and acetone have critical temperatures only slightly >500 K. At temperatures near the critical temperature, the vapor pressure of probes could be higher than the atmospheric pressure and gradually approaching the critical pressure. The saturated vapor of probes would depart from the ideal gas state. Because IGC is generally operated near one atmosphere pressure and permanent gases are used as the carrier gas, there is a tendency to think that the vapor phase is in an ideal gas state. This is not true for probe vapors. This departure from the ideal gas state for probes have two effects on the solution thermodynamic properties. The first is the effect on the activity coefficient of probes. The reference state for the activity coefficient of probes is the fugacity of the saturated liquid state.[34] An increase in vapor pressure of a probe will affect the activity coefficient of the probe. This effect was considered in early studies on the IGC method[6,7] and is corrected by the last term of eq. (1). In their derivation, it was assumed that the departure of

the probe vapor from the ideal gas state can be described by the second viral coefficient. Because this term is proportional to the vapor pressure of probes, its effect is significant even when permanent gases such as helium or nitrogen are used as the carrier gas. With this correction, the activity coefficient and χ determined by the IGC method are considered to be the zero pressure value.[6,7]

The second effect occurs when χ is used in the determination of δ_2 by using eqs. (2) and (6). It is the effect of the departure of vapor phase of probes from the ideal gas state on the solubility parameter of probes, δ_i. In the original concept of cohesive energy density, it is the energy required to separate molecules into the ideal gas state. The definition in eq. (2), however, gave only the heat of vaporization. At temperatures near the critical temperature, the density of the vapor phase gradually increases, and the departure of saturated vapor from the ideal gas state becomes significant and needs to be included in the definition of cohesive energy density. The effect of high temperature on cohesive energy density, and the need to include a vapor phase correction to estimate the solubility parameter, was noticed in the literature.[13,35] Tan and Munk[35] obtained a correlation for vapor phase cohesive energy based on the second virial coefficient. Naik and Aminabhavi compared three methods to δ_i in an IGC study of polystyrene.[33] These methods applied the corresponding-states correlations by using reduced temperature (T_r), reduced pressure (P_r), and acentric factor (ω) to calculate the solubility parameter of a liquid. In this study, the cohesive energy density is separated into the heat of vaporization and departure of vapor from the ideal gas state to facilitate the assessment of the effect of vapor phase departure. Heat of vaporization of many compounds was recently compiled by Yaws.[36,37] The departure of vapor from the ideal gas can be estimated by using corresponding-states correlations.

There are two objectives in this study. First, an error in the solubility parameter of probes, δ_i, will cause an error in the determination of the solubility parameter of the polymer, δ_2. In the previous study,[19] this author derived a formula to give the effect of a deviation of χ from the solubility parameter model on the determination of δ_2. Likewise, a similar effect would happen when δ_i was in error. Second, it was pointed out that the use of probes with a range of δ_i on both sides of δ_2 can reduce the correlation between η and δ_2. Most probes in IGC studies had δ_i lower than δ_2. To have $\delta_i > \delta_2$ would necessitate the use of polar probes. These effects will be demonstrated by using systems at high temperature and with probes on both sides of δ_2.

RESULTS AND DISCUSSION

Solubility parameter of probes

To illustrate the procedure and make a comparison, IGC data of nine probes in poly(ε-caprolactone) (PCL)

and poly(hydroxyl ether of bisphenol A) (PH) measured by Juana et al.[38] were used in this study. Polymer samples of de Juana et al. were obtained from commercial sources: PCL (Polyscience, Niles, IL) and PH (Quimidroga, Barcelona, Spain). PCL had $M_n = 10,800$ and $M_w = 17,600$. PH had $M_n = 18,000$ and $M_w = 50,700$. De Juana et al. measured the specific retention volumes of probes in PCL and PH and blends at weight ratios of 25/75, 50/50, and 75/25 at temperatures of 130–160°C. The mixtures were miscible and gave negative polymer–polymer interaction parameters. The interaction parameters of probes in both polymers at 150°C were reported and will be used in this study to determine the solubility parameters of the polymers. This information was used because it was measured at a higher temperature and used probes with different strengths of δ_i, covering from hydrocarbon to alcohol. Many studies on solubility parameters of polymers used only probes with a limited solubility parameter range (e.g., n-alkanes and aromatics). In the previous study,[19] it was pointed out that the confidence interval of parameters of the polymers is inverse to the variance of δ_i used. A wide range of δ_i is preferred for the determination of δ_2.

To make a linear plot using eq. (6), the solubility parameters of probes at high temperatures needed to be calculated. Several correlation methods were used to estimate the parameters of probes. The enthalpy of vaporization is calculated by

$$\Delta H_{\text{vap}} = A(1 - T/Tc)^n \qquad (8)$$

This relation is known as the Waston equation.[39] T_c is the critical temperature. The exponent n is generally around 0.38. The parameters A and n of many chemical compounds are available in Yaws[36] and on the Internet.[37] This equation predicts that the heat of vaporization of a saturated liquid decrease when temperature increases and becomes zero at the critical temperature. However, the cohesive energy of a probe vapor is not zero at the critical point. The solubility parameter of probes in eq. (2) was defined for a low vapor pressure situation. Near the critical temperature, the saturated vapor is in a high-temperature and high-density state and its internal energy departure from the ideal state, $(E^0 - E)_{\text{vap}}$, should be combined with the heat of vaporization for the calculation of solubility parameter. The formula then becomes

$$\delta^2 = [\Delta E_{\text{vap}} + (E° - E)_{\text{vapor}}]/V_{\text{liquid}} = [\Delta H_{\text{vap}} + (H° - H)_{\text{vapor}} - (RT - PV_{\text{liquid}})]/V_{\text{liquid}} \qquad (9)$$

From the reduced vapor pressure and critical compressibility factor, Z_c, the enthalpy departure of the saturated vapor, $H^0 - H$, was calculated based on the method of Yen and Alexander.[40,41] In this method, the

TABLE I
Properties of Probes at 150°C

Probe	V	P°	Pr	Tr	δ	δ–δ*
n-Decane	226.95	0.52	0.024	0.684	13.25	0.14
l-Butanol	107.81	2.77	0.062	0.751	18.84	0.31
Chloroform	99.44	10.16	0.183	0.789	15.38	1.00
Toluene	125.23	2.70	0.065	0.715	15.25	0.42
Benzene	106.69	5.72	0.115	0.752	15.00	0.72
1,2-Dichloroethane	94.98	5.50	0.101	0.754	16.75	0.64
Chlorobenzene	117.13	1.57	0.034	0.669	16.64	0.21
3-Pentanone	128.10	3.50	0.092	0.754	14.81	0.37
Propyl acetate	140.02	3.61	0.106	0.770	14.32	0.50

Note. Molar volume (V = cm^3/mol), vapor pressure (P° = bar), reduced pressure (Pr), reduced temperature (Tr), solubility parameter with vapor phase correction δ = (J/cm^3)$^{0.5}$, and without the vapor phase correction δ*.

dimensional ratio $(H^0 - H)/T_c$ (in units of cal/g mol) was correlated to the reduced vapor pressure, $P_{\text{sat},r}$, for several Z_c. For the case of $Z_c = 0.25$, the following expression was given:

$$(H° - H)/Tc = 6.5P_{\text{sat},r}^{0.62252}/(1 + 0.76218$$
$$(- \ln P_{\text{sat},r})^{0.536042}) \quad (10)$$

Different coefficients were given for Z_c at 0.23, 0.25, 0.27, and 0.29. For probe with a Z_c different from the above values, an interpolation method was used by using two nearby Z_c's. The molar volume required in eq. (9) was calculated by using density, ρ, estimated by the following equation of Yaws:[36,37]

$$\rho = AB^{-(1-Tr)^n} \quad (11)$$

where T_r (=T/T_c) is the reduced temperature. The parameters A, B, and n, which are different from those in eq. (8), are available in Yaws[36] and on the Internet.[37] The vapor pressure of probes was also calculated by using the equation

$$\log_{10}(P_{\text{vap}}) = a + b/T + c \log_{10}(T) + dT + eT^2 \quad (12)$$

where P_{vap} is the vapor pressure in mmHg, T is temperature in Kelvin, and the parameters a, b, c, d, and e are also available from Yaws[36] and on the Internet.[37] From this information, the cohesive energy and the solubility parameter of probes were calculated.

The solubility parameters of probes, δ_i, at 150°C are shown in Table I. A symbol δ* is used in this study to indicate the solubility parameters of the probes without the vapor phase correction and the parameters of polymers calculated from them. The values of $\delta - \delta$* are also listed in Table I. Also shown in Table I are reduced temperatures and reduced pressures data. It can be seen that, when T_r was 0.789 as in the case of chloroform, the difference in solubility parameter

reached 1.00 (J/cm^3)$^{0.5}$. Figure 1 shows the difference, $\delta - \delta$*, versus the reduced temperature of probes. It can be seen that $\delta - \delta$* increased as the temperature increased. The deviation increases more rapidly as temperature approaches T_c. Equation (8) predicts that the heat of vaporization is zero at T_c, but the departure of enthalpy from eq. (10) gives a finite value. Estimated by eq. (10) with typical values of $V_c = 300$ cm^3/mol and $T_c = 550$ K, the solubility parameter could reach 7 (J/cm^3)$^{0.5}$ at T_c. Because the solubility parameter of most organic liquids is about 20 (J/cm^3)$^{0.5}$ at room temperature, the vapor still retains about one-third of the value at T_c. It is interesting to point out that even at temperatures above T_c, a gas can still have solubility in liquids and a solubility parameter can be assigned. Steinberg and Manowitz[42] determined the solubility parameter of Xenon at 25°C by the solubility in different liquids. Therefore, it is reasonable that a solubility parameter can be assigned to a probe even at a temperature near T_c. The vapor phase nonideality provides the cohesive energy of a vapor.

Figure 2 shows the linear plot of eq. (6) for PCL at 150°C. A comparison was made by using the solubility parameter without vapor phase correction. The solubility parameter of the polymer was determined to be 16.35 and 15.67 (cal/cm^3)$^{0.5}$ for δ_2 and δ_2*, respectively. The difference $\delta_2 - \delta_2$* is in the range of $\delta_i - \delta_i$* of probes. It can be seen that, when correction was made, the solubility parameter of probes increased. It also increased the left-hand side of eq. (6). The two lines were almost overlapped because a change in δ_i also changed the δ_i^2/RT term. This represents the correlation effect between the left-hand side of eq. (6) and δ_i, which was pointed out in the previous study.[19] A vertical shift was applied to separate the two lines in Figure 2. The overall effect is a small increase of the slope as seen in the slope of two regression lines. In
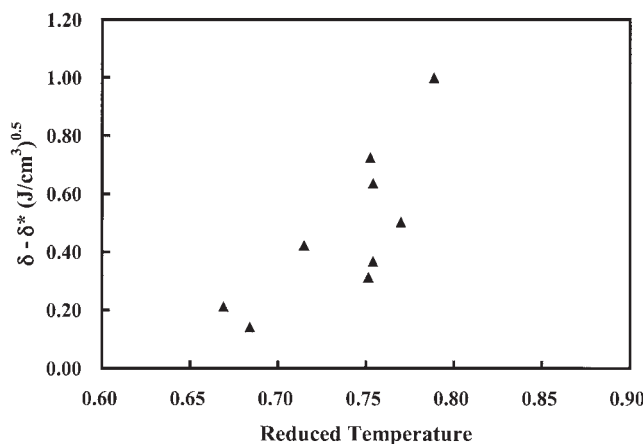

Figure 1 Error of the solubility parameters of probes due to the vapor phase nonideality at 150°C versus reduced temperature.
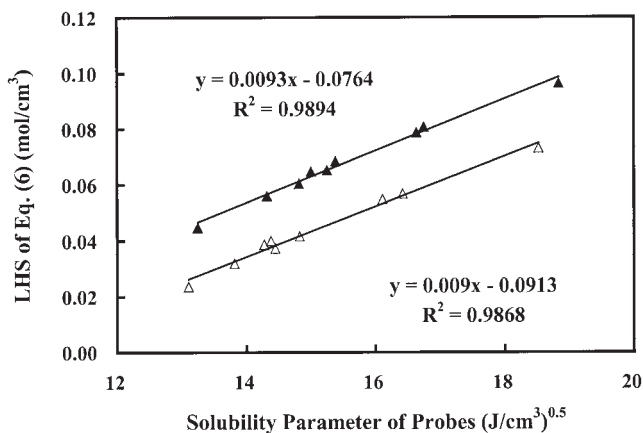
Figure 2 The plot of left-hand side of eq. (6) versus the solubility parameters of probes in PCL at 150°C. Open symbols are without vapor phase correction; filled symbols are with vapor phase correction. Open symbols were shifted downward by 0.02 mol/cm³.

both plots, the correlation coefficients (R^2) based on the linear regression method was close to unity. It was 0.9868 when δ^* was used and 0.9894 when δ was used. The correction in vapor phase nonideality increased R^2. Figure 3 shows the similar result for PH. Again, the correction of vapor phase nonideality gave a higher solubility parameter for the polymer and a higher R^2. PH had smaller δ_2 and δ_2^* compared to PCL.

Comparison of RTχ/V with prediction

In a recent study, the author pointed out the dominating effect of the δ_i^2/RT term on the left-hand side of eq. (6) and proposed a direct method to determine δ_2 and η by rearranging eq. (6) into the form[19]
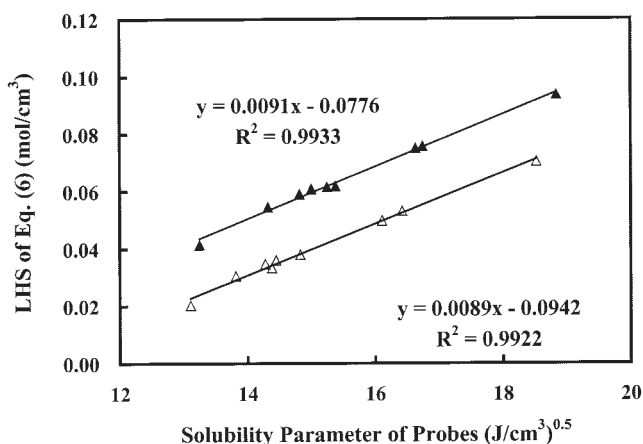

Figure 3 The plot of left-hand side of eq. (6) versus the solubility parameters of probes in PH at 150°C. Open symbols are without vapor phase correction; filled symbols are with vapor phase correction. Open symbols were shifted downward by 0.02 mol/cm³.
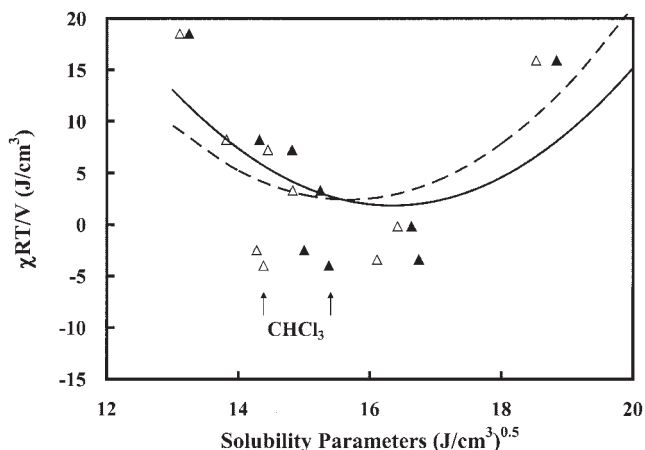

Figure 4 Comparison of experimental $RT\chi/V$ with the solubility parameter model for probes in PCL at 150°C. Open symbols and dashed curve are without vapor phase correction; filled symbols and solid curve are with vapor phase correction.

$$RT\chi/V_i = (\delta_i - \delta_2)^2 + RT\chi_s/V_i = (\delta_i - \delta_2)^2 + RT\ \eta + \lambda_i \quad (13)$$

where η is the average value of χ_S/V_i and is assumed to be constant for a polymer as in the linear plotting method; λ_i is the error in fitting the model. Equation (13) is a nonlinear model with two parameters, δ_2 and η. The summation of error square (SS) for a series of probes with solubility parameter, δ_i, molar volume, V_i, and interaction parameter, χ_i, is

$$SS = \Sigma\lambda_i^2 = \Sigma[RT\chi/V_i - (\delta_i - \delta_2)^2 - RT\ \eta]^2 \quad (14)$$

Setting the partial differentiations $\partial(SS)/\partial\delta_2$ and $\partial(SS)/\partial\eta$ to be zero, the expressions for the optimum value of δ_2 and η were obtained. It was concluded that the expression of the δ_2 term was the same as eq. (7) but the result of η had a different expression:[19]

$$\eta = [\Sigma\chi_i/V_i - \Sigma(\delta_i - \delta_2)^2/RT]/N \quad (15)$$

where N is the number of probes, δ_2 is the solubility parameter of the polymer, and the summation is taken for all the probes. Figure 4 compares the experimental values of $RT\chi/V$ with the model in eq. (13) for PCL at 150°C. Also shown in the figure is the result using solubility parameters of probes without the vapor phase correction. The predicted values, using eq. (13) and calculated as δ_2 and η, were plotted as solid curves. Another dashed curve represents the result by using δ^*. The effect of the vapor phase correction was to make the curve shift toward the right-hand side and increase δ_2. The η term decreased slightly when the vapor phase correction was made. The effect of vapor phase correction can be clearly seen in Figure 4 by the
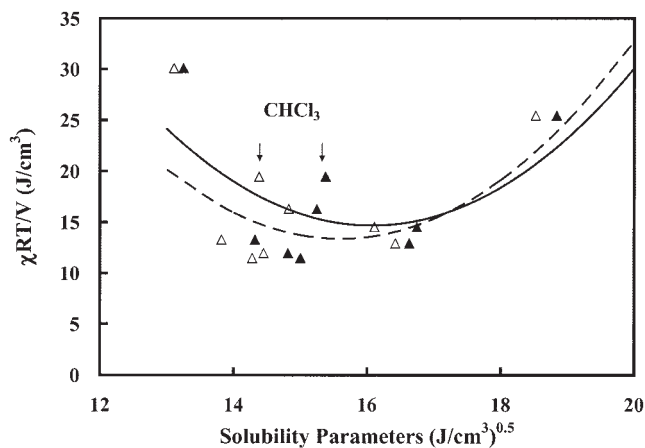
Figure 5 Comparison of experimental $RT\chi/V$ with the solubility parameter model for probes in PH at 150°C. Open symbols and dashed curve are without vapor phase correction; filled symbols and solid curve are with vapor phase correction.

moving of the points. Figure 5 shows a similar result for PH. The effect of vapor phase correction also increased δ_2, but a decrease in η was seen. It appeared that an increase in δ_i can lead to either an increase or a decrease of η.

The values of δ_2 and η for both polymers are shown in Table II. The values of η were lower for PCL. It is noted that PCL in the previous study[19] also had an η value near zero at 80°C. The lower value of PCH probably results from the specific interaction with the probes. The probe that made the most moves is chloroform. It is shown in both Figures 4 and 5. It had a high negative deviation in Figure 4 but had a high positive deviation in Figure 5. This is a result of a specific interaction between chloroform and PCL. The hydrogen bonding between the hydrogen of chloroform and the carbonyl group of PCL does not exist in PH. In PH, hydrogen bonding is formed between the hydroxyl groups of PH. The hydroxyl groups of PH tend to associate with each other[38] rather than interacting with probes and make χ of all probes higher than PCL.

TABLE II
Results from Curve Fitting of eq. (13) at 150°C

	PCL	PH
δ_2 $(J/cm^3)^{0.5}$	16.35	16.07
δ_2^* $(J/cm^3)^{0.5}$	15.67	15.60
$RT\eta$ (J/cm^3)	1.85	14.67
$RT\eta^*$ (J/cm^3)	2.42	13.03
ψ	0.146	0.222
S_R (J^2/cm^6)	243.52	146.54

Note. δ_2^* and η^* are parameters of polymer determined using probes without vapor phase correction.

TABLE III
Parameters for the Approximate Joint Confidence Region and the Confidence Interval (CI)

	PCL	PH
$\bar{\delta}-\delta_2$ $(J/cm^3)^{0.5}$	−0.764	−0.493
A_{11} (J/cm^3)	105.76	93.5
A_{12}, A_{21} (J/cm^3)	224.72	142.59
A_{22} (J/cm^3)	2404.43	2325.36
90% CI of $\delta_{2,0}$ $(J/cm^3)^{0.5}$	1.643	1.328
90% CI of $RT\Delta\eta_0/\delta_{2,0}$ $(J/cm^3)^{0.5}$	0.306	0.231
Angle of inclination	−5.5°	−3.6°

In the previous study,[19] the following dimensionless ratio was proposed to estimate the goodness of fit for eq. (13):

$$\psi = \Sigma(y_{est} - \bar{y})^2/\Sigma(y - \bar{y})^2 \quad (16)$$

where y represents the experimental value of $RT\chi_i/V_i$, $\bar{y}$ is the average value of all probes, and y_{est} is the estimated value of the left-hand side of eq. (13) using the calculated δ_2 and η. The symbol ψ is used in this article instead of R^2 so that it would not be confused with the R^2 in Figures 2 and 3. Equation (16) gives the ratio between the variance of predicted values and experimental values. The values shown in Table II were less than unity. These indicated that the variances of experimental values were higher than the predicted values, and the ratio was smaller than unity even though a reasonable fit was seen visually in Figures 4 and 5. The use of eq. (16) is more rigorous than R^2 in Figures 2 and 3. The ratio is closer to unity for PH because it has less deviation. Another quantity that can be used to compare the model is the sum-of-error square. It is given as S_R in Table II. It was higher for PCL because it had more deviations than PH, as seen in Figures 4 and 5.

Sensitivity of δ_2 and η to the solubility parameter of probes

Without the vapor phase correction, the solubility parameter of probes tends to be lower. This deviation can affect the determination of δ_2 and η. It is important to be able to estimate the error in the determination of δ_2 when this error happens. The effect of the error term, $\Delta\delta_i$, on δ_2 can be derived from eq. (7) by taking the derivative of $\ln \delta_2$ versus δ_i

$$\partial \ln\delta_2/\partial\delta_i = (1/\delta_2)(\partial\delta_2/\partial\delta_i) = [2\delta_i(\delta_i - \bar{\delta}) + (\delta_i^2$$
$$- RT\chi_i/V_i) - (1/N)\Sigma(\delta_i^2 - RT\chi_i/V_i)]/\Sigma(\delta_i - \bar{\delta})(\delta_i^2$$
$$- RT\chi_i/V_i) - 2(\delta_i - \bar{\delta})/\Sigma(\delta_i - \bar{\delta})^2 = [2\delta_i(\delta_i - \bar{\delta}) + (\delta_i^2$$
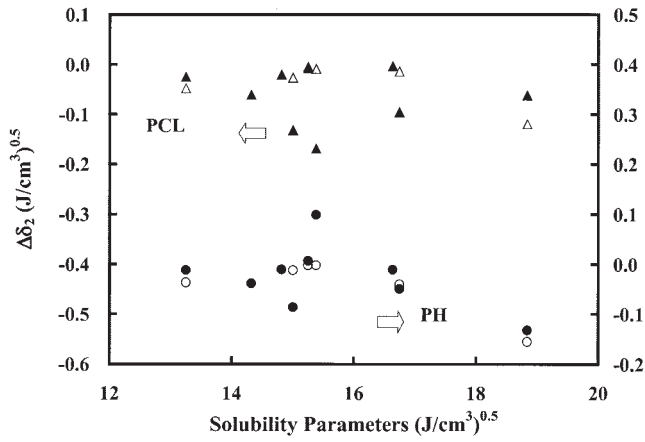
Figure 6 The effect of $\Delta\delta_2$, caused by $\Delta\delta_i$ of probes, versus solubility parameter of probes for PCL and PH at 150°C. Filled symbols represent the total value; open symbols represent the effect of the first term in eq. (18).

$$- RT\chi_i/V_i) - (1/N)\Sigma(\delta_i^2 - RT\chi_i/V_i)]/[2\delta_2\Sigma(\delta_i - \bar{\delta})^2]$$
$$- 2(\delta_i - \bar{\delta})/\Sigma(\delta_i - \bar{\delta})^2 \quad (17)$$

The equation can be modified by using eq. (13) to give

$$\Delta\delta_2 = (\partial\delta_2/\partial\delta_i)\Delta\delta_i = [2(\delta_i - \bar{\delta})(\delta_i - \delta_2)$$
$$- \lambda_i]\Delta\delta_i/2[\Sigma(\delta_i - \bar{\delta})^2] = (\delta_i - \bar{\delta})(\delta_i - \delta_2)\Delta\delta_i/(N$$
$$- 1)\sigma^2 - \lambda_i\Delta\delta_i/2(N - 1)\sigma^2 \quad (18)$$

where σ^2 is the sample variance of δ_i. When $\Delta\delta_i$ is a constant for all probes, the summation of $\Delta\delta_2$ is the constant $\Delta\delta_i$. This agrees with the physical meaning that the curve is moved horizontally by a constant value without a vertical motion. Equation (18) shows that $\Delta\delta_2$ contains two parts. The first part is proportional to $(\delta_i - \bar{\delta})(\delta_i - \delta_2)$. For a probe with $\delta_i < \bar{\delta}$ and $\delta_i < \delta_2$, an increase of δ_i tends to increase δ_2. The same result happens when $\delta_i > \bar{\delta}$ and $\delta_i > \delta_2$. When δ_i is near $\bar{\delta}$ or δ_2, the effect is small because the probe is located at the horizontal portion of the parabolic curves. Thus, for a probe at the far left or right ends of the probe distribution, a decrease in δ_i will result in a decrease of δ_2. The second part of eq. (18) occurs from the error term in the solubility parameter model, λ_i. For many probes, the λ_i term contributes more than the first term. Because λ_i can be either positive or negative for a particular probe, $\Delta\delta_2$ can be positive even though $\Delta\delta_i$ is negative. We can call $\Delta\delta_2$ the sensitivity factor of a probe toward the value of δ_2.

Figure 6 shows the plot of $\Delta\delta_2$ and the first term of eq. (18) versus the solubility parameter of probes. The difference between them represents the effect of the second term. The effect of the first term resembles a parabolic function because the effect is higher at both

ends as pointed out in the previous paragraph. The data point out that the most left-hand side deviates from the trend. The point represents n-decane, which has the smallest $\Delta\delta_i$. With the inclusion of the second term, the overall effect showed that probes at both ends had a small $\Delta\delta_2$ and probes at the center had a wider range of $\Delta\delta_2$. This is because the probes at the center had a higher $\Delta\delta_i$, and the effect of the λ_i term was also large. This is different from the previous study[19] on the effect of the deviation of χ from the solubility parameter model on $\Delta\delta_2$. In the case of the deviation of χ, the probes near the center made only a small contribution because $\Delta\delta_2$ was weighted by a small $(\bar{\delta} - \delta_i)$. In Figure 6, the largest effect was made by chloroform. This is because it had the highest $\Delta\delta_i$. It is noted that the $\Delta\delta_2$ of chloroform had different signs in the two polymers because of a difference in sign of the λ_i term, which can also be seen in Figures 4 and 5. This represents a specific interaction between chloroform and PCL and its absence in PH. In most probes, $\Delta\delta_2$ was negative because $\Delta\delta_i$ was also negative. Therefore, the effect of $\Delta\delta_2$ from each probe is cumulative. If more probes with high T_r were used, the total effect could be important.

The effect of the error term, $\Delta\delta_i$, on η was derived from eqs. (7) and (18):

$$RT\Delta\eta = RT(\partial\eta/\partial\delta_i)\Delta\delta_i + RT(\partial\eta/\partial\delta_2)(\partial\delta_2/\partial\delta_i)\Delta\delta_i$$
$$= 2(\delta_2 - \delta_i)\Delta\delta_i/N + (\bar{\delta} - \delta_2)[2(\delta_i - \bar{\delta})(\delta_i - \delta_2)$$
$$- \lambda_i]\Delta\delta_i/(N - 1)\sigma^2 \quad (19)$$

Equation (19) shows that $RT\Delta\eta$ depends on two terms. The first term represents the direct effect of $\Delta\delta_i$ on η. The second term occurs because there is a dependency between η and δ_2 in eq. (15). The deviation term, $\Delta\delta_i$, affected δ_2, which in turn affected η. When $\Delta\delta_i$ is a constant for all probes, the summation of $RT\Delta\eta$ is zero. This agrees with the physical meaning that the curve is moved horizontally by a constant value without a vertical motion. When $\Delta\delta_i$ is not a constant, the summation of $RT\Delta\eta$ would not be zero.

Figure 7 shows the plot of $RT\Delta\eta$ and $2(\delta_2 - \delta_i)\Delta\delta_i/N$ versus the solubility parameters of probes for both polymers. The difference between $RT\Delta\eta$ and $2(\delta_2 - \delta_i)\Delta\delta_i/N$ represents the contribution from the last term in eq. (19). Similarly to Figure 6, some probes in the center region showed a wider deviation than the probes at both ends. In both polymers, the second term gave a positive contribution to $RT\Delta\eta$ for most probes. The effect was smaller in PH. The second term is proportional to $(\bar{\delta} - \delta_2)$, which is the result of the dependency of η on δ_2. The value of $(\bar{\delta} - \delta_2)$ is -0.764 and -0.493 $(J/cm^3)^{0.5}$ for PCL and PH, respectively. This difference accounted for the difference in the magnitude of the last term of eq. (19). When probes
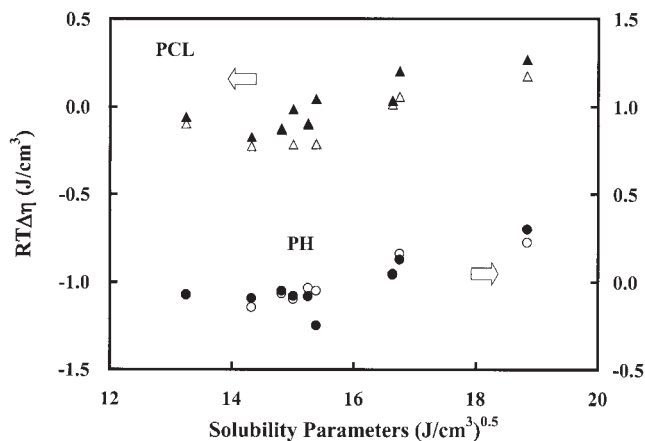
Figure 7 The effect of $RT\Delta\eta$, caused by $\Delta\delta_i$ of probes, versus solubility parameter of probes for PCL and PH at 150°C. Filled symbols represent the total value; open symbols represent the effect of the first term in eq. (19).

with $\bar{\delta} = \delta_2$ are used, the second term is zero because there is no correlation between η and δ_2, as explained in the previous study.[19] Because $RT\Delta\eta$ varied from negative to positive when δ_i increased, a large portion of $RT\Delta\eta$ by different probes cancelled and the overall effect was small. The mathematical meaning is that the horizontal moving of points in Figures 4 and 5 only move the curve slightly in the vertical direction.

Confidence intervals of parameters

By using a linearization method[43] around the optimum values of the two parameters, $\delta_{2,0}$ and η_0, the approximate joint confidence region for the summation of error square, $\Sigma \lambda_i^2$, can be expressed as a quadratic form of two variables $[X_1, X_2] = [\delta_2 - \delta_{2,0}, (\eta - \eta_0)RT/\delta_{2,0}]$:

$$A_{11}X_1^2 + 2A_{12}X_1X_2 + A_{22}X_2^2 = S_R\frac{p}{N-p}F_\alpha(N, N-p)$$

$$(20)$$

where S_R is the sum of error square (SS) calculated at the optimum values $\delta_{2,0}$ and η_0 using eq. (14), F_α is the F distribution with confidence level α, p is the number of parameters, and N is the number of samples. The reason that $\eta RT/\delta_{2,0}$ was used as the variable instead of η was to make the dimensions of both variables consistent. For this study, $p = 2$, $N = 9$, and the F_α at 90% confidence level is 3.26. The coefficients A_{11}, A_{12}, and A_{22} can be determined from the partial differentiation with respect to SS by using the expression in eq. (14):

$$A_{11} = (1/2)\partial^2(SS)/\partial X_1^2 = 4\Sigma(\delta_i - \delta_{2,0})^2 \quad (21)$$

$$A_{12} = A_{21} = (1/2)(\delta_{2,0}/RT)\partial^2(SS)/\partial X_1\partial X_2$$

$$= -2\Sigma(\delta_i - \delta_{2,0})\delta_{2,0} \quad (22)$$

$$A_{22} = (1/2)(\delta_{2,0}/RT)^2\partial^2(SS)/\partial X_2^2 = N\delta_{2,0}^2 \quad (23)$$

The values of A_{11}, A_{12}, and A_{22} are listed in Table III. The 90% joint confidence regions were ellipses and are shown in Figure 8. The angle of inclination listed in Table III indicates that the joint confident region is only slightly oblique and there is little correlation between δ_2 and η. It was pointed out in the previous study[19] that the dependence of δ_2 on η in eq. (15) was the cause of correlation. Because $\partial\eta/\partial\delta_2$ is proportional to $(\bar{\delta} - \delta_2)$, there is no correlation when $(\bar{\delta} - \delta_2)$ is zero. The correlation can be compared by the magnitude of $(\bar{\delta} - \delta_2)$, which was also listed in Table III. In the previous study,[19] the angle of inclination for PCL at 80°C was about $-15°$ when probes were located at the left-hand side of δ_2. The ellipses had a higher inclination than those in this study. The difference $(\bar{\delta} - \delta_2)$ was -3.20 $(J/cm^3)^{0.5}$, which differed from zero more than the values in this study.

Finally, the coefficient matrix can be transformed into a diagonalized form and the confidence interval (CI) of variables can be calculated from the length of the principal axes of ellipses. The parameters for the joint confidence region of PCL and PH are listed in Table III. The 90% CI of PCL is longer than PH because the former has a higher S_R. The 90% CI of PCL is longer than that of PCL in the previous study[19] because fewer probes were used in this study (i.e., 9 versus 25). The value of 1.64 $(J/cm^3)^{0.5}$ for CI in this study is a large value, considering that the solubility parameters of most organic compounds only range from 14 to 20 $(J/cm^3)^{0.5}$, as shown in Table I. If fewer samples or probes with narrow δ_i are used, the CI will
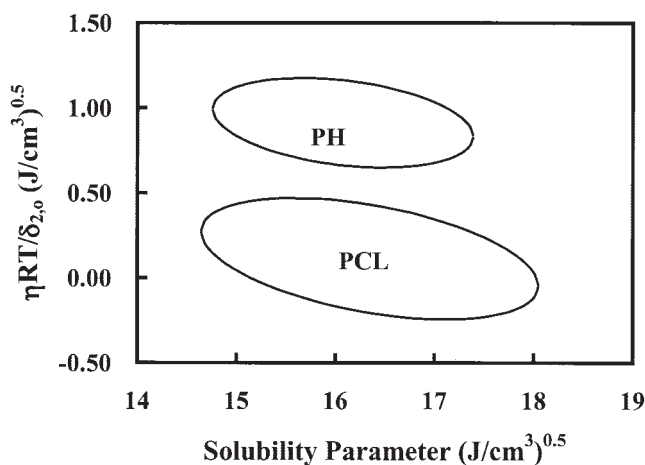

Figure 8 Approximate joint confidence region of δ_2 and $\eta RT/\delta_{2,0}$ at 90% level for PCL and PH.

be even wider. This study demonstrated the importance of testing CI of parameters.

CONCLUSION

A method is proposed to include a correction for the nonideality of the vapor phase of probes in the determination of solubility parameter of polymers at high temperature. By using PCL and PH and nine probes at 150°C as an example, it was found that, without the correction, the solubility parameters of probes and polymers tended to be underestimated. Formulae were derived to estimate the error of the parameters in the solubility parameter model caused by the correction term. The CIs of parameters were calculated. The use of more probes with a wider solubility parameter range can reduce the CI of the parameters. Selecting probes with $\bar{\delta}$ near δ_2 can reduce the correlation between δ_2 and η.

References

1. Conder, J. R.; Young, C. L. Physicochemical Measurement by Gas Chromatography; Wiley: New York, 1979.
2. Laub, R. J.; Pescok, P. L. Physicochemical Applications of Gas Chromatography; Wiley: New York, 1978.
3. Al-Saigh, Z. Y.; Guillet, J. E. in Meyers, R., Ed.; Encyclopedia of Analytical Chemistry: Instrumentation and Applications; Wiley: Chichester, 2000; p. 7759.
4. Vilcu, R.; Leca, M. Polymer Thermodynamics by Gas Chromatography, translated by V. Vasilescu; Elsevier: Amsterdam, 1990.
5. Langer, S. H.; Sheehan, R. J.; Huang, J.-C. J Phys Chem 1982, 86, 4605.
6. Everett, D. H. Trans Faraday Soc 1965, 61, 1637.
7. Gruickshank, A. J. B.; Windsor, M. L.; Young, C. L. Proc R Soc Lond A 1966, 295, 259.
8. Flory, P. J. Principles of Polymer Chemistry; Cornell University Press: Ithaca, NY, 1953.
9. Smidsrod, O.; Guillet, J. E. Macromolecules 1969, 2, 272.
10. Guillet, J. E. J Macromol Sci Chem 1970, 4, 1669.
11. Hildebrand, J. H. J Am Chem Soc 1916, 38, 1452.
12. Scatchard, G. Chem Rev 1931, 8, 321.
13. Hildebrand, J. H.; Prausnitz, J. M.; Scott, R. L. Regulated and Related Solutions; Van Nostrand Reinhold Co.: New York, 1970.
14. DiPaola-Baranyi, G.; Guillet, J. E. Macromolecules 1978, 11, 228.
15. Ito, K.; Guillet, J. E. Macromolecules 1979, 12, 1163.
16. Scott, R. L.; Magat, M. J Chem Phys 1945, 13, 172.
17. Scott, R. L.; Magat, M. J Polym Sci 1949, 4, 555.
18. Huang, J.-C. J Appl Polym Sci 2003, 89, 1242.
19. Huang, J.-C. J Appl Polym Sci 2004, 91, 2894.
20. Galin, M. Polymer 1983, 24, 865.
21. Aspler, J. S.; Gray, D. G. Polymer 1982, 23, 43.
22. Eguiazabal, J. I.; Fernandez-Berridi, M. J.; Iruin, J. J.; Elorza, J. M. Polym Bull (Berl) 1985, 13, 463.
23. Merk, W.; Lichtenthaler, R. N.; Prausnitz, J. M. J. Phys Chem 1980, 84, 1694.
24. Price, G. J. Polym Mater Sci Eng 1985, 58, 1009.
25. Humpa, O.; Uhdeova, J.; Roth, M. Macromolecules 1991, 24, 2514.
26. Roth, M. Macromolecules 1990, 23, 1696.
27. Barton, A. F. M. Handbook of Polymer-Liquid Interaction Parameters and Solubility Parameters; CRC Press: Boston, 1990.
28. Su, A. C.; Fried, J. R., in Lloyd, D. R.; Ward, T. C.; Schreiber, H. P., Eds.; Inverse Gas Chromatography: Characterisation of Polymers and Other Materials; ACS Symposium Series No. 391; Chapter 12; American Chemical Society: Washington, DC, 1989.
29. Kaya, I.; Ozdemir, E. Polymer 1999, 40, 2405.
30. Kaya, I.; Demirelli, K. Polymer 2000, 41, 2853.
31. Becerra, M. R.; Fernandez-Snachez, E.; Fernandez-Torres, J. A.; Garcia-Dominguez, J. A.; Santiuste, J. M. Macromolecules 1992, 25, 4665.
32. Kong, X.; Silveria, M. D. L. V.; Zhao, L.; Choi, P. Macromolecules 2002, 35, 8586.
33. Naik, H. G.; Aminabhavi, T. M. J Appl Polym Sci 2001, 80, 1291.
34. Prausnitz, J. M. Molecular Thermodynamics of Fluid-Phase Equilibria; Prentice-Hall: Upper Saddle River, NJ, 1969.
35. Tan, M.; Munk, P. J. J Solution Chem 1995, 24, 267.
36. Yaws, C. L. Yaws' Handbook of Thermodynamic and Physical Properties of Chemical Compounds: Physical, Thermodynamic and Transport Properties for 5,000 Organic Chemical Compounds; Knovel: Norwich, NY, 2003.
37. www.knovel.com.
38. de Juana, E.; Etxeberris, A.; Cortazar, M.; Iruin, J. J. Macromolecules 1994, 27, 1395.
39. Thek, R. E.; Stiel, L. I. AIChE J 1966, 12, 599; AIChE J 1967, 13, 626.
40. Reid, R. C.; Prausnitz, J. M.; Sherwood, T. K. The Properties of Gases and Liquids, 3rd ed.; McGraw-Hill, New York, 1977; p. 115.
41. Yen, L. C.; Alexander, R. E. AIChE J 1965, 11, 334.
42. Steinberg, M.; Manowtiz, B. Ind. Eng Chem 1959, 51, 49.
43. Draper, N. R.; Smith, H. Applied Regression Analysis, 2nd ed.; Wiley: New York, 1981; Chapter 10.